

# AB-INITIO CALCULATIONS OF THE DIELECTRIC CONSTANT, OPTICAL ABSORPTION AND THE REFRACTIVE INDEX OF $Zn_{1-x}Be_xO$ ALLOY

SAID LAKEL<sup>(1,2)</sup>, FATIMA ELHAMRA<sup>(2)</sup>, M. IBRIR<sup>(3)</sup>, K. ALMI<sup>(1)</sup>

<sup>(1)</sup>Laboratory of physical materials - University of LAGHOUAT – BP 37G, Laghouat, Algeria

<sup>(2)</sup>Laboratory of Metallic and Semiconducting Materials, University of Biskra, Algeria

<sup>(3)</sup>Laboratory of Physics of Materials and its Applications, University of Msila, Algeria.

E-mail: s.lakel@yahoo.fr

## ABSTRACT

The optical properties of  $Zn_{1-x}Be_xO$  were studied by first principle method using the density functional theory. The dielectric function and optical constants are calculated using PP-PW method within the generalized gradient approximation (GGA). The theoretical calculated optical properties yield a static dielectric constant for  $Zn_{1-x}Be_xO$  are 4.08, 3.86, 3.60, 3.12 and 2.85 along polarization direction (001). It indicates that the static dielectric constants reduce with increasing Be concentration. However a static refractive indices for  $Zn_{1-x}Be_xO$  are found to be 2.05, 1.98, 1.88, 1.77 and 1.70 with the increasing x, respectively. The obtained results agree well with the available theoretical and experimental values.

**KEYWORDS:** Optical Properties, refractive index, PP-PW, DFT.

## 1 INTRODUCTION

The ZnO is a kind of wide band gap semiconductor and an attractive material due to its use in ultraviolet optoelectronic applications, solar cells [1], sensors [2], nano lasers [3,4], etc. To produce high efficiency ZnO-based light emitting devices, the critical step is the fabrication of quantum wells and super lattices of ZnO-based semiconductor alloys by mixing with materials with even larger band gaps.

$Zn_{1-x}Be_xO$  has advantages over  $Zn_{1-x}Mg_xO$  and  $Zn_{1-x}Cd_xO$ , because BeO has the same hexagonal wurtzite structure as ZnO, phase segregation is not detected in  $Zn_{1-x}Be_xO$  alloys [5,6,7].

In order to design active regions for LEDs, a barrier material with energy gap larger than ZnO is needed, and both MgZnO and BeZnO are possible choices. Although MgZnO is technologically more mature, BeZnO may potentially offer some advantages. In fact, since BeO and ZnO have the same hexagonal symmetry, phase segregation in BeZnO is a far less critical issue than in MgZnO and, in principle, the energy band gap of BeZnO can be engineered to range from 3.4 eV (ZnO) to 10.6 eV (BeO) by changing the Be molar fraction. This makes it is possible to grow barrier layers with higher confinement than those obtained with MgZnO, potentially leading to better performance in the deep-UV spectral range. Ryu and co-workers [7,8] [8,9]

have shown that it is indeed possible to grow BeZnO-based LED and laser structures. Therefore, it is important to provide the ZnO community with a preliminary evaluation of the BeZnO potential as a LED material. Such applications, in turn, require an accurate determination of the structural, electronic and optical properties and of

$Zn_{1-x}Be_xO$ .

In the present work the optical properties of  $Zn_{1-x}Be_xO$  have been studied using the pseudo potential plane wave method (PP-PW). The results, in comparison with the published data, are in good agreement with the experimental and previous theoretical results.

## 2 COMPUTATIONAL METHODS

Our calculations were performed by the Cambridge Serial Total Energy Package (CASTEP) program [9], which is the implementation of the conserving pseudo-potential method. [10]. The method is based on the density functional theory. The exchange correlation potential is treated by the generalized gradient approximation (GGA) with the Perdew-Wang functional [11, 12]. The  $Zn_{1-x}Be_xO$  ( $x = 0.0, 0.25, 0.5, 0.75, 1.0$ ) structures can be obtained by replacing 1 to 8 Zn atoms with Be in the  $2 \times 2 \times 1$  wurtzite ZnO supercell. We used a plane-wave basis set defined by an

energy cut-off 600 eV. We used 6X6 Monkhorst mesh [13] to sample the first Brillouin zone. The structural parameters are determined using the Broyden– Fletcher–Goldfarb–Shenno (BFGS) minimization technique [14]. The total energy is stable within 5 eV/atom, the maximum ionic Hellmann–Feynman force is less than 10 eV/Å.

The complex dielectric tensor was calculated, in this program, according to the well-known relations [15].

$$\varepsilon_2(\omega) = \frac{4\pi^2 e^2}{m^2 \omega^2} \sum \int \langle i | M | j \rangle^2 f_i (1 - f_j) \times \delta[E_f - E_i - \omega] d^3K \quad (1)$$

$$\varepsilon_1(\omega) = 1 + \frac{2}{\pi} P \int_0^{\infty} \frac{\omega' \varepsilon_2(\omega')}{\omega^2 - \omega'^2} d\omega' \quad (2)$$

And the optical conductivity is given by:

$$Re \sigma_{\alpha\beta}(\omega) = \frac{\omega}{4\pi} \text{Im} \varepsilon_{\alpha\beta}(\omega) \quad (3)$$

In Equation (1),  $ck$  and  $vk$  are the crystal wave functions corresponding to the conduction and the valence bands with crystal wave vector  $k$ . In Equation (3) the conductivity tensor relating the inter band current density  $j_\alpha$  in the direction  $\alpha$  which flows upon application of an electric field  $E_\beta$  in direction  $\beta$  in which the sum in Equation (1) is over

all valence and conduction band states labeled by  $v$  and  $c$ .

Moreover, the complex dielectric constant of a solid is given as:

$$\varepsilon(\omega) = \varepsilon_1(\omega) + i \varepsilon_2(\omega) \quad (4)$$

Here, real and imaginary parts are related to optical constants  $n(\omega)$  and  $k(\omega)$  as:

$$\begin{aligned} \varepsilon_1(\omega) &= n^2(\omega) - k^2(\omega) \\ \varepsilon_2(\omega) &= 2n(\omega)k(\omega) \end{aligned} \quad (5)$$

The other optical parameters, such as energy-loss spectrum and oscillator strength sum rule are immediately calculated in terms of the components of the complex dielectric function [16].

### 3 RESULT AND DISCUSSIONS

The unit cell of wurtzite structure is characterized by three parameters, the lattice constant  $a$ , the  $c/a$  ratio, and the internal parameter  $u$  which fixes the relative position of the anion and cation sub-lattices along the  $c$  axis. Table 1 displays the calculated structural parameters of the equilibrium configurations of  $\text{Zn}_{1-x}\text{Be}_x\text{O}$ .

The results listed in Table 1 show that the lattice constants,  $a$  and  $c$ , decrease with an increase in beryllium composition. This phenomenon occurs because the atom radius of beryllium is smaller than that of zinc.

**Table 1: Calculated equilibrium lattice constants  $a$  and  $c$  of  $\text{Zn}_{1-x}\text{Be}_x\text{O}$  compared with both theoretical and experimental data**

x	a (Å)			c (Å)		
	This work	expt.	other calculations	This work	expt.	other calculations
1	2.614	2.698 <sup>a</sup>	2.764 <sup>b</sup>	4.255	4.377 <sup>a</sup>	4.487 <sup>b</sup>
0.75	2.81		2.889 <sup>b</sup>	4.525		4.675 <sup>b</sup>
0.5	2.912		2.972 <sup>b</sup>	5.01		4.99 <sup>b</sup>
0.25	3.112		3.134 <sup>b</sup>	5.094		5.076 <sup>b</sup>
0	3.262	3.258 <sup>d</sup>	3.283 <sup>b</sup> , 3.256 <sup>c</sup>	5.28	5.22 <sup>d</sup>	5.309 <sup>b</sup> , 5.256 <sup>c</sup>

<sup>a</sup> Ref.[17], <sup>b</sup>Ref.[18], <sup>c</sup>Ref.[19], <sup>d</sup>Ref.[20]

#### 3.1 Dielectric function

The calculated optical properties at the equilibrium lattice constant are illustrated in detail in the present work. The results have been presented in Figs. 1-4. It is well known that the imaginary part of the dielectric function  $\varepsilon_2(\omega)$  can be treated by the transitions between occupied and

unoccupied electronic states. The real part  $\varepsilon_1(\omega)$  and imaginary part  $\varepsilon_2(\omega)$  along polarization direction (001) for  $\text{Zn}_{1-x}\text{Be}_x\text{O}$  are displayed in Figs. 1 and 2. It is clear that the calculated values of ZnO and BeO are in reasonable agreement with those available in literature [21,22]. An important quantity of  $\varepsilon_1(\omega)$  is the zero frequency limit  $\varepsilon_1(0)$ , which depends on the band gap as  $\varepsilon_1(0) \approx 1 + (\hbar\omega_p/E_g)^2$ ,

where  $\omega_p$  is the plasma frequency at which  $\epsilon_1(\omega)$  passes through zero [23]. The Zn<sub>1-x</sub>Be<sub>x</sub>O has the similar characteristic in the static dielectric constant  $\epsilon_1(0)$  changing with the molar fraction  $x$  along polarization direction (001). Our calculated static dielectric constants for Zn<sub>1-x</sub>Be<sub>x</sub>O are 4.08, 3.86, 3.60, 3.12 and 2.85 along polarization direction (001). It indicates that the static dielectric constants are reduced with increasing Be concentration. In the range 0-12 eV, as  $x$  increases, the first strong peak in  $\epsilon_1(\omega)$  shifts toward higher incident photon energy, which varies from 3.36 eV in ZnO to 10.55 eV in BeO along polarization direction (001). From Fig. 2, it is noted that ZnO has a strong absorption region which starts from 1.35 eV to 21.5 eV along polarization direction (001) while BeO has less region of strong absorption.

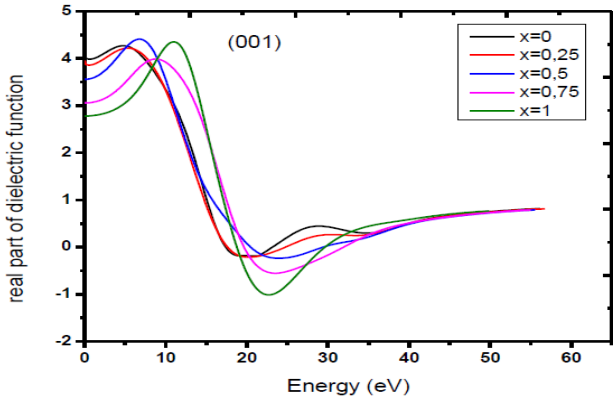


Figure1: Real part of dielectric function of Zn<sub>1-x</sub>Be<sub>x</sub>O alloys

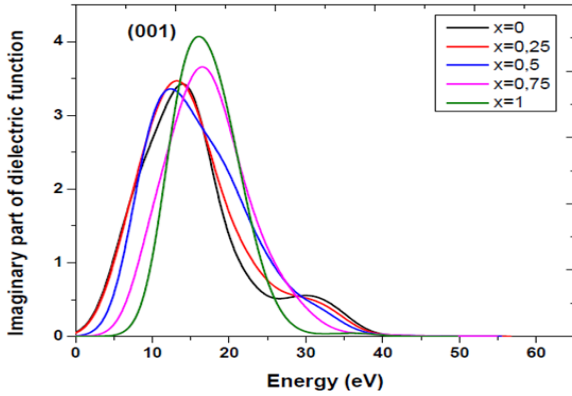


Figure2: Imaginary part  $\epsilon_2(\omega)$  of dielectric function of Zn<sub>1-x</sub>Be<sub>x</sub>O alloys

### 3.2 Optical absorption

The variation of absorption with increasing concentration of Be in Zn<sub>1-x</sub>Be<sub>x</sub>O is shown in Fig. 3 along polarization direction (001). The shape of the optical absorption is the most important, which shows a sharp onset followed by an almost plateau. The absorption edge starts at about 1.55, 1.98, 4.12, 4.88 and 7.28 eV, respectively. It is noticed that a high absorption peak occurs in ZnO in the energy range of 12-20 eV and the peak shifts toward lower energy as the concentration of Be increases.

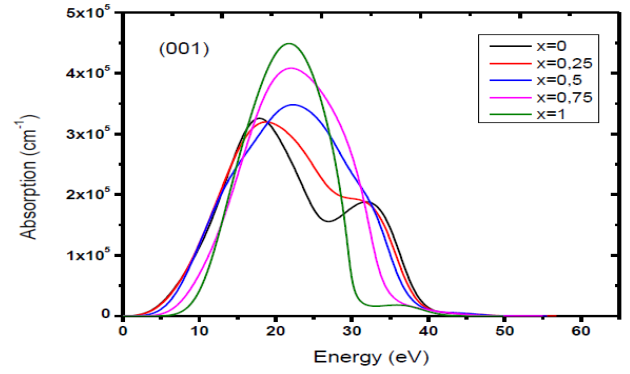


Figure3: Variation of absorption of Zn<sub>1-x</sub>Be<sub>x</sub>O alloys a long (001) direction

### 3.3 Refractive Index

The refractive index of material is an important optical parameter, which is often required to interpret various types of spectroscopic data. It is related to the density and the local polarizability of these entities [24]. The refractive index of a semiconductor  $n(\omega)$  is computed through the real dielectric function  $n = \sqrt{\epsilon_1(\omega)}$ . The part of the refractive index is presented in Fig. 4 and refractive indices  $n(0)$  for Zn<sub>1-x</sub>Be<sub>x</sub>O are found to be 2.05, 1.98, 1.88, 1.77 and 1.70 with the increasing  $x$ , respectively. The refractive index was measured to be 1.72 along c-axis for BeO [25], showing an excellent agreement with our calculated value.

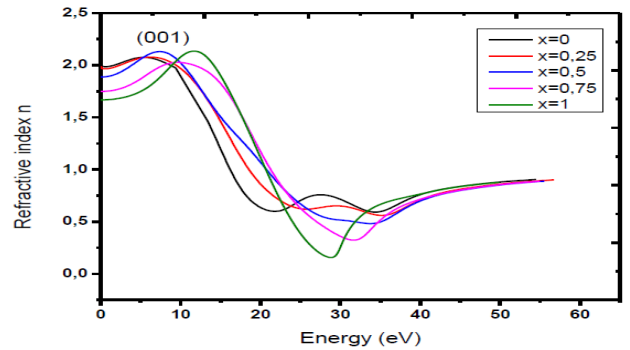


Figure4: Variation of refractive index of Zn<sub>1-x</sub>Be<sub>x</sub>O alloys along (001) direction

## 4 CONCLUSION

In summary, the equilibrium structure, and optical properties of Zn<sub>1-x</sub>Be<sub>x</sub>O alloys are discussed in detail. The obtained lattice constants indicated a close agreement with the reported experimental values and literature data. For polarization direction (001), the absorption edge starts at about 1.55, 1.98, 4.12, 4.88 and 7.28 eV, respectively. It is noticed that a high absorption peak occurs in ZnO in the energy range of 12-20. eV and the peak shifts towards lower energy as the concentration of Be increases. The refractive indices  $n(0)$  for Zn<sub>1-x</sub>Be<sub>x</sub>O are found to be 2.05,

1.98, 1.88, 1.77 and 1.70 with the increasing  $x$ , respectively.

## REFERENCES

- [1] K. Keis, E. Magnusson, H. Lindström, S.-E. Lindquist, A. Hagfeldt, *Solar energy materials and solar cells* 73 (1) (2002) 51–58.
- [2] N. Golego, S. A. Studenikin and M. Cocivera, *J. Electrochem. Soc.*, 147 (2000) 1592–1594.
- [3] M.H. Huang, S. Mao, H. Feick, H. Yan, Y. Wu, H. Kind, E. Weber, R. Russo, P. Yang *Science* 292 (2001) 1897—1899.
- [4] J.C. Johnson, H. Yan, R.D. Schaller, L.H. Haber, R.J. Saykally and P. Yang, *Single nanowire lasers*, *J. Phys. Chem. B*, 105(2001) 11387.
- [5] M. Sanati, G. L.W. Hart and A. Zunger 2003 *Phys. Rev. B* 68 155210.
- [6] A. Ohtomo, M. Kawasaki, I. Ohkubo, H. Koinuma, T. Yasuda and Y. Segawa 1999 *Appl. Phys. Lett.* 75 980.
- [7] Y. R.Ryu, T. S. Lee, J. A. Lubguban, A.B.Corman, H. W. White, J. H. Leem, M. S. Han, Y. S. Park, C. J. Youn and W J Kim 2006 *Wide-band gap oxide alloy: BeZnO* *Appl. Phys. Lett.* 88 052103.
- [8] W. J. Kim, J. H. Leem, M. S. Han, I.W. Park, Y. R. Ryu and T. S. Lee, 2006 *J. Appl. Phys.* 99 096104.
- [9] M.D. Segall, P.J.D. Lindan, M.J. Probert, C.J. Pickard, P.J. Hasnip, S.J. Clark, M.C. Payne, *J. Phys.: Condens. Mat.* 14 (2002) 2717.
- [10] W. Kohn, L. Sham, *Phys. Rev. A* 140 (1965) 1133.
- [11] P.L. Mao, B. Yu, Z. Liu, F. Wang, Y. Ju, *J. Magn. Alloy* 1 (2013) 256.
- [12] D.M. Ceperley, B.J. Alder, *Phys. Rev. Lett.* 45 (1980) 566.
- [13] J.P. Perdew, A. Zunger, *Phys. Rev. B* 23 (1981) 5048.
- [14] D.R. Hamann, M. Schluter, C. Chiang, *Phys. Rev. Lett* 43 (1979) 1494–1497.
- [15] F. Wooten, “*Optical properties of solids*,” Academic Press, New York, 1972.
- [16] S. Loughin, R H French, L K De Noyer, W-Y Ching and Y-N Xu, *Journal of Physics D: Applied Physics*, Vol. 29(1996) 1740-1750.
- [17] F. Decremps, F. Datchi, A.M. Saitta, A. Polian, S. Pascarelli, A.D. Cicco, J.P. Itie, F. Baudelet, *Phys. Rev. B* 68 (2003) 104101.
- [18] A. Schleife, F. Fuchs, J. Furthmüller, F. Bechstedt, *Phys. Rev. B* 73(2006) 245212.
- [19] Zheng Yongping, Chen Zhigao, Lu Yu, Wu Qingyun, Weng Zhenzhen and Huang Zhigao. *J. Semicond* 29(12) , 2316-2321 (2008).
- [20] R.M. Hazen, L.W. Finger, *J. Appl. Phys.* 59 (1986) 3728.
- [21] S. Nazir, N. Ikrama, B. Amin, M. Tanveer, A. Shaukat and Y Saeed 2009 *J. Phys. and Chem. of Solid.* 70 874.
- [22] D.Groh, R. Pandey, M.B. Sahariah, E. Amzallag, I Baraille and R. Merat M 2009 *J. Phys. and Chem. of Solid.* 70 789.
- [23] Penn D R 1962 *Phys. Rev.* 128 2093.
- [24] R. Goldhahn, J. Scheiner, S. Shokhovets, T Frey, U Ko Ehler, D. J. As and K. Lischkam 1999 *Phys. Status Solidi (B)* 216 265.
- [25] Yen T S, Kuo C K, Han W L, Qui Y H and Huang Y Z 1983 *J. Am. Ceram. Soc.* 66 860.